

# 000 QUAD: Q-GRADIENT UNCERTAINTY-AWARE GUID- 001 ANCE FOR DIFFUSION POLICIES IN OFFLINE REIN- 002 FORCEMENT LEARNING

003  
004  
005  
006 **Anonymous authors**  
007 Paper under double-blind review  
008  
009  
010  
011  
012

## ABSTRACT

013 Diffusion-based offline reinforcement learning (RL) leverages Q-gradients of  
014 noisy actions to guide the denoising process. Existing approaches fall into two  
015 categories: (i) backpropagating the Q-gradient of the final denoised action through  
016 all steps, or (ii) directly estimating the Q-gradient of noisy actions. The former  
017 suffers from exploding or vanishing gradients as the number of denoising steps  
018 increases, while the latter becomes inaccurate when noisy actions deviate substan-  
019 tially from the dataset. In this work, we focus on addressing the limitations of the  
020 second category. We introduce QUAD, an uncertainty-aware Q-gradient guidance  
021 method. QUAD employs a Q-ensemble to estimate the uncertainty of Q-gradients  
022 and uses this uncertainty to constrain unreliable guidance during denoising. By  
023 down-weighting unreliable gradients, QUAD reduces the risk of producing sub-  
024 optimal actions. Experiments on the D4RL benchmark show that QUAD outper-  
025 forms state-of-the-art methods across most tasks.  
026

## 1 INTRODUCTION

027 Reinforcement learning (RL) has achieved remarkable progress in sequential decision-making tasks,  
028 ranging from games (Mnih et al., 2013; Lample & Chaplot, 2017) to robotics (He et al., 2024b; Ze  
029 et al., 2025). However, the majority of these successes rely heavily on abundant online interac-  
030 tions. In many real-world domains, such as healthcare, autonomous driving, and industrial con-  
031 trol, exploration is either prohibitively costly or inherently unsafe. Offline RL addresses this chal-  
032 lenge by learning policies purely from pre-collected datasets (Fujimoto & Gu, 2021; Zhou et al.,  
033 2025), thereby eliminating the need for online exploration. However, it suffers from distribution  
034 shift (Levine et al., 2020): the learned policy may produce actions that deviate substantially from  
035 those observed in the dataset, resulting in unreliable value estimates and degraded performance. A  
036 key contributor to this issue is the limited expressiveness of conventional policy classes (e.g. Gaus-  
037 sian), which struggle to capture complex, multimodal action distributions in real-world datasets,  
038 worsening the mismatch between learned and behavior policies.  
039

040 Diffusion models (Ho et al., 2020) have emerged as a powerful class of policies (Chi et al., 2023),  
041 capable of capturing highly complex action distributions and generating diverse actions. Diffusion-  
042 based offline RL methods typically combines two forms of guidance: behavior cloning (BC) guid-  
043 ance and Q-guidance (Wang et al., 2022). BC guidance steers the denoising trajectory towards  
044 dataset-like actions, thereby alleviating distributional shift, whereas Q-guidance leverages value es-  
045 timates to promote higher-quality actions. Existing Q-guidance methods can be categorized into  
046 two classes. The first backpropagates Q-gradients from the final denoised action through all diffu-  
047 sion steps (Wang et al., 2022). While effective in principle, this approach suffers from vanishing  
048 or exploding gradients as the number of denoising steps increases, leading to unstable optimization.  
049 The second estimates Q-gradients of noisy actions directly at intermediate denoising steps (Fang  
050 et al., 2024), thus avoiding backpropagation through the entire trajectory. Although more stable,  
051 this method produces unreliable Q-gradients when noisy actions lie far from the data distribution,  
052 resulting in suboptimal guidance.  
053

To address the limitations of the second class of methods, we propose **QUAD**, a Q-gradient  
uncertainty-aware guidance framework that improves the reliability of denoising guidance. Our

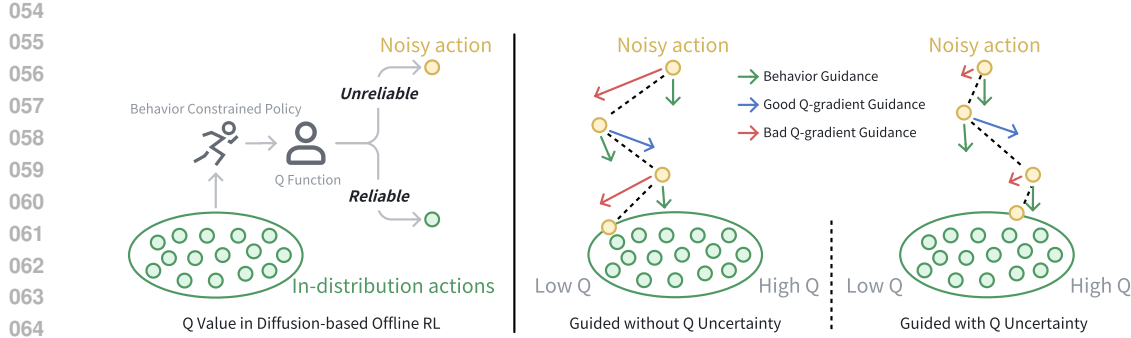


Figure 1: Left: In offline RL, behavior cloning regularization makes the learned Q-function more reliable near the dataset distribution (green), while yielding highly uncertain estimates for out-of-distribution noisy actions (orange). Right: QUAD leverages a Q-ensemble to estimate the uncertainty of Q-gradients and adaptively down-weights unreliable guidance during denoising.

key observation is that critics trained on offline data often yield highly unreliable Q estimates for noisy actions, particularly those far from the dataset distribution (Figure 1, left). To overcome this issue, QUAD employs a Q-ensemble to estimate gradient uncertainty and adaptively attenuate unreliable guidance signals (Figure 1, right). We further provide a theoretical analysis of Q-gradient uncertainty and derive an optimal weighting scheme that minimizes the alignment risk along oracle Q-gradient. Building on this analysis, we design a practical uncertainty-aware weighting mechanism that approximates the theoretical optimum. By integrating this mechanism into the Q-guidance process, QUAD effectively suppresses unreliable gradients, thereby enhancing policy performance.

We evaluate QUAD on the widely adopted D4RL benchmark (Fu et al., 2020), comparing it against state-of-the-art offline RL methods, including both non-diffusion and diffusion-based approaches. Experimental results show that QUAD consistently outperforms prior methods on most tasks and achieves comparable performance on the remaining ones.

In summary, our contributions are threefold:

- We identify and theoretically analyze the limitations of existing Q-guidance methods in diffusion-based offline RL, showing how Q-gradient uncertainty undermines reliability.
- We propose **QUAD**, a novel uncertainty-aware guidance framework that leverages a Q-ensemble to estimate gradient uncertainty and adaptively down-weight unreliable signals.
- We conduct extensive experiments on D4RL, demonstrating that QUAD achieves state-of-the-art performance across a diverse set of offline RL tasks.

## 2 PRELIMINARIES

A reinforcement learning (RL) problem is typically formulated as a Markov Decision Process (MDP), represented by the tuple  $(\mathcal{S}, \mathcal{A}, \mathcal{T}, r, d_0, \gamma)$ , where  $\mathcal{S}$  denotes the state space,  $\mathcal{A}$  the action space,  $\mathcal{T}(s'|s, a)$  the transition dynamics,  $r(s, a)$  the reward function,  $d_0(s)$  the initial state distribution, and  $\gamma \in (0, 1)$  the discount factor. The objective of RL is to learn a policy  $\pi(a|s)$  that maximizes the expected discounted cumulative reward (Sutton et al., 1998):

$$J(\pi) = \mathbb{E}_{\pi, \mathcal{T}, d_0} \left[ \sum_{t=0}^{\infty} \gamma^t r(s_t, a_t) \right] \quad (1)$$

**Offline Reinforcement Learning.** Offline RL focuses on learning an effective policy solely from a fixed dataset  $\mathcal{D} = \{(s_i, a_i, r_i, s'_i)\}_{i=1}^N$ , which is generated by an (often unknown) behavior policy  $\pi_\beta$ , without access to further environment interactions (Levine et al., 2020). A central challenge in offline RL arises from the distributional shift between  $\pi_\beta$  and the learned policy  $\pi$ , which can lead

108 to erroneous value estimates. To mitigate this issue, many approaches optimize the expected return  
 109 under  $Q^\pi(s, a)$  while constraining the learned policy to remain close to the behavior policy (Wu  
 110 et al., 2019):

$$111 \quad \max_{\pi} \mathbb{E}_{s \sim \mathcal{D}, a \sim \pi(\cdot|s)} [Q^\pi(s, a)] \quad \text{s.t.} \quad D(\pi \| \pi_\beta) < \epsilon \quad (2)$$

112 where  $D(\cdot, \cdot)$  denotes a divergence measure (e.g., KL divergence) and  $\epsilon$  is a tolerance parameter.  
 113

114 **Diffusion models.** Diffusion models (Ho et al., 2020; Song et al., 2020a) are a class of generative  
 115 models that assume latent variables follow a Markovian noising-denoising process. In the forward  
 116 process  $\{x_{0:T}\}$ , Gaussian noise is gradually added to the clean data  $x_0 \sim p(x_0)$  according to a  
 117 predefined variance schedule  $\{\beta_{1:T}\}$ :

$$118 \quad q(x_{1:T}|x_0) = \prod_{t=1}^T q(x_t|x_{t-1}), \quad q(x_t|x_{t-1}) := \mathcal{N}(x_t; \sqrt{1 - \beta_t}x_{t-1}, \beta_t \mathbf{I}) \quad (3)$$

121 The marginal distribution admits a closed form:

$$122 \quad q_t(x_t|x_0) = \mathcal{N}(x_t; \sqrt{\bar{\alpha}_t}x_0, (1 - \bar{\alpha}_t)\mathbf{I}), \quad t \in \{1, \dots, T\} \quad (4)$$

123 where  $\alpha_t := 1 - \beta_t$  and  $\bar{\alpha}_t := \prod_{s=1}^t \alpha_s$ . Equivalently, a noisy sample can be reparameterized as  
 124

$$125 \quad x_t = \sqrt{\bar{\alpha}_t}x_0 + \sqrt{1 - \bar{\alpha}_t} \epsilon, \quad \epsilon \sim \mathcal{N}(\mathbf{0}, \mathbf{I}) \quad (5)$$

126 Denoising diffusion probabilistic models (DDPMs) (Ho et al., 2020) parameterize the reverse pro-  
 127 cess with Gaussian conditionals  $p_\theta(x_{t-1}|x_t) = \mathcal{N}(x_{t-1}; \mu_\theta(x_t, t), \Sigma_\theta(x_t, t))$ , leading to a genera-  
 128 tive process:  $p_\theta(x_{0:T}) = \mathcal{N}(x_T; \mathbf{0}, \mathbf{I}) \prod_{t=1}^T p_\theta(x_{t-1}|x_t)$ . In practice, DDPMs predict the noise  $\epsilon$  in  
 129 Equation (5) using a neural network  $\epsilon_\theta(x_t, t)$  to minimize the evidence lower bound loss:

$$130 \quad \mathcal{L}(\theta) = \mathbb{E}_{x_0 \sim p(x_0), t \sim \mathcal{U}(1, T), \epsilon \sim \mathcal{N}(\mathbf{0}, \mathbf{I})} [\|\epsilon - \epsilon_\theta(x_t, t)\|^2] \quad (6)$$

131 **Diffusion-based Offline RL.** Following the DDPM framework, diffusion policies model action gen-  
 132 eration as a state-conditioned denoising process. Specifically, the noise predictor in (Equation (6)) is  
 133 replaced with a state-conditional network  $\epsilon_\theta(a^t, s, t)$  that predicts actions  $a^0 \in \mathcal{A}$  given the state  $s$ ,  
 134 where  $a^t$  denotes the noisy action at denoising step  $t$ . This formulation recovers standard behavior  
 135 cloning (BC) when trained on the dataset  $\mathcal{D}$ . In diffusion-based offline RL, however, pure behav-  
 136 ior cloning may fail to exploit Q value information. To address this, Q-function guidance can be  
 137 incorporated to bias the denoising process toward high-value actions. A straightforward approach,  
 138 as in Diffusion Q-learning (DQL) (Wang et al., 2022), backpropagates the Q-gradient from the final  
 139 denoised action  $a^0$  through all denoising steps, leading to the following objective:

$$140 \quad \arg \min_{\pi_\theta} \mathcal{L}(\theta) = \mathbb{E}_{(s, a) \sim \mathcal{D}, t \sim \mathcal{U}(1, T), \epsilon \sim \mathcal{N}(\mathbf{0}, \mathbf{I})} [\|\epsilon - \epsilon_\theta(a^t, s, t)\|^2] \\ 141 \quad - \eta \cdot \mathbb{E}_{s \sim \mathcal{D}, a^0 \sim \pi_\theta} [Q_\phi(s, a^0)] \quad (7)$$

142 where the first term corresponds to the denoising objective, and the second term encourages the  
 143 policy to generate actions with high Q-values. The coefficient  $\eta$  is a hyperparameter that balances  
 144 behavior cloning against Q-guidance. An alternative strategy, as in DAC (Fang et al., 2024), directly  
 145 estimates the Q-gradient of noisy actions at each denoising step, leading to the following objective:

$$147 \quad \arg \min_{\pi_\theta} \mathcal{L}(\theta) = \mathbb{E}_{(s, a) \sim \mathcal{D}, t \sim \mathcal{U}(1, T), \epsilon \sim \mathcal{N}(\mathbf{0}, \mathbf{I})} [\eta \cdot \|\epsilon - \epsilon_\theta(a^t, s, t)\|^2 \\ 148 \quad + w(t) \cdot \epsilon_\theta(a^t, s, t) \cdot \nabla_{a^t} Q_\phi(s, a^t)] \quad (8)$$

149 where  $w(t)$  is a step-dependent weight that controls the influence of Q-gradient guidance across  
 150 denoising steps. Rather than propagating gradients across the full sequence of denoising steps,  
 151 DAC-style methods reduce the risk of vanishing or exploding gradients, thereby providing more  
 152 stable optimization.

### 155 3 METHODS

158 We now introduce our proposed method, QUAD, which comprises three main components: (1) a  
 159 theoretical derivation of an uncertainty-aware weighting scheme for Q-gradient guidance; (2) the  
 160 formulation and implementation of a Q-gradient uncertainty-aware guidance mechanism; and (3) a  
 161 practical yet principled procedure for policy extraction. An overview of the QUAD framework is  
 162 shown in Figure 2.

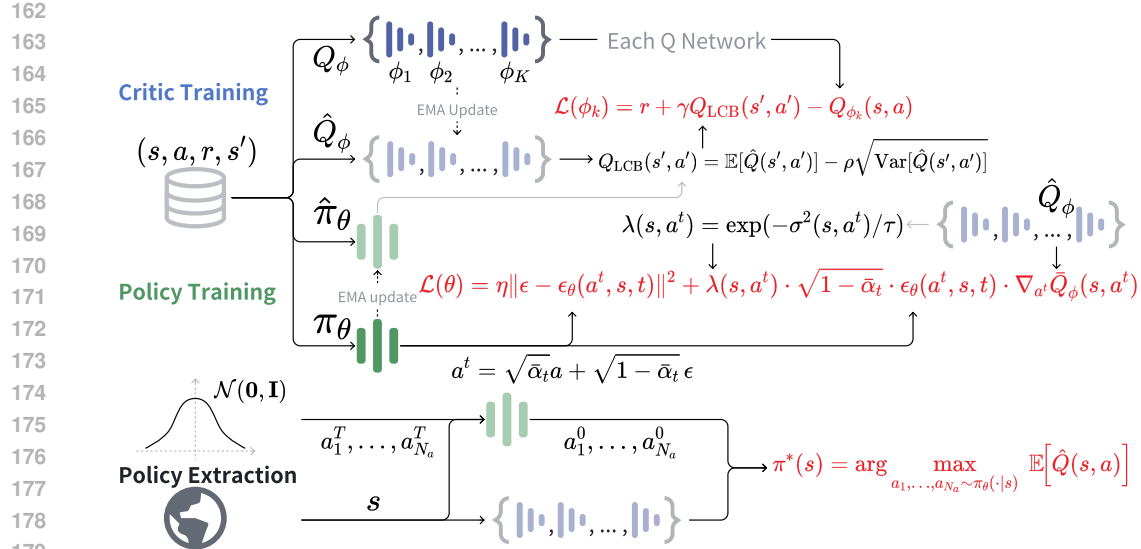


Figure 2: Overview of the QUAD framework: (1) In critic ensemble training, the target policy generates next-step actions and updates critics by minimizing TD error with LCB regularization. (2) In diffusion policy training, the target Q-ensemble estimates Q-gradients and their uncertainty to adaptively down-weight unreliable guidance. (3) In policy extraction, the target diffusion policy proposes candidate actions, and the action with the highest Q-value under the target Q-ensemble is selected.

### 3.1 THEORETICAL ANALYSIS OF Q-GRADIENT UNCERTAINTY-AWARE WEIGHTING

#### 3.1.1 Q-GRADIENT UNCERTAINTY AND OPTIMAL WEIGHTING

For convenience, we denote the oracle Q-gradient as  $\mathbf{g}^* = \nabla_{\mathbf{a}^t} Q^*(\mathbf{s}, \mathbf{a}^t)$ . In the ideal case, the second term in Equation (8) encourages  $\epsilon_\theta$  to align with  $-\mathbf{g}^*$ , and we define the alignment loss via their inner product:

$$g^* \triangleq \epsilon_\theta \cdot \mathbf{g}^*. \quad (9)$$

However, we can only access an approximation of  $\mathbf{g}^*$ , denoted as  $\mathbf{g}_\phi = \nabla_{\mathbf{a}^t} Q_\phi(\mathbf{s}, \mathbf{a}^t)$ . Its alignment loss along  $\epsilon_\theta$  is written as

$$g_\phi \triangleq \epsilon_\theta \cdot \mathbf{g}_\phi. \quad (10)$$

We assume (see Appendix A) that  $\mathbf{g}_\phi$  follows the biased-noisy decomposition:

$$\mathbf{g}_\phi = \mathbf{g}^* + \mathbf{b} + \boldsymbol{\xi}_\phi, \quad (11)$$

where  $\mathbf{b}$  is a deterministic bias determined only by the offline dataset and the learning algorithm, and  $\boldsymbol{\xi}_\phi$  is a zero-mean random noise with finite covariance, arising from stochastic function approximation and training randomness rather than from the fixed data or algorithm design. Their alignment losses along  $\epsilon_\theta$  are

$$b \triangleq \epsilon_\theta \cdot \mathbf{b}, \quad \boldsymbol{\xi}_\phi \triangleq \epsilon_\theta \cdot \boldsymbol{\xi}_\phi,$$

so that

$$g_\phi = \mathbf{g}^* + b + \boldsymbol{\xi}_\phi. \quad (12)$$

The combined term  $b + \boldsymbol{\xi}_\phi$  captures the epistemic uncertainty of the Q-gradient induced by limited offline data and critic approximation, which we refer to as the **Q-gradient uncertainty**. Let  $\sigma^2(\mathbf{s}, \mathbf{a}^t, t) = \text{Var}(\boldsymbol{\xi}_\phi)$  denote the variance of this random alignment noise at  $(\mathbf{s}, \mathbf{a}^t, t)$ .

Although we cannot directly reduce the Q-gradient uncertainty, we can mitigate the risk of using  $g_\phi$  in the alignment loss. We define the alignment risk as the expected squared error between  $g_\phi$  and  $g^*$ :

$$\mathcal{R} \triangleq \mathbb{E}[(g_\phi - g^*)^2], \quad (13)$$

216 where the expectation is taken over the randomness in  $\xi_\phi$ . To reduce this risk, we introduce a per-  
 217 sample weighting factor  $\lambda(\mathbf{s}, \mathbf{a}^t, t)$  and consider the risk of the weighted alignment loss:  
 218

$$219 \quad \mathcal{R}(\lambda) \triangleq \mathbb{E}[(\lambda g_\phi - g^*)^2]. \quad (14)$$

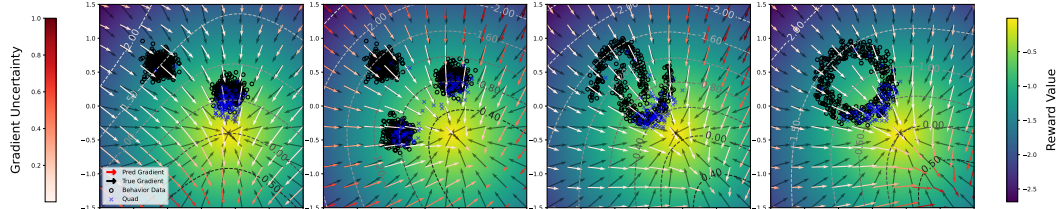
220 Under the biased–noisy model above, the **optimal weighting** that minimizes  $\mathcal{R}(\lambda)$  admits the  
 221 closed-form solution (details see Appendix A)

$$222 \quad \lambda^*(\mathbf{s}, \mathbf{a}^t, t) = \frac{g^*(g^* + b)}{(g^* + b)^2 + \sigma^2(\mathbf{s}, \mathbf{a}^t, t)}. \quad (15)$$

225 The sign structure of the oracle and biased term plays a crucial role:  
 226

- 227 • If  $g^*$  and  $g^* + b$  have the same sign (the approximate critic is directionally aligned), then  
 228  $\lambda^* \in (0, 1)$  and behaves as a shrinkage factor.
- 229 • If they have opposite signs (directionally misaligned), then  $\lambda^*$  may become negative or  
 230 larger than 1, which is not reliably implementable without oracle access.

231 These two regimes are illustrated on a toy bandit example in Figure 3, where the wrong-direction  
 232 regime exhibits large variance and strong disagreement across critics. This motivates the variance-  
 233 only weighting strategy used in QUAD, described next.  
 234



235  
 236 Figure 3: Bandit examples under four different data distributions: the highest reward is located  
 237 at point  $(0.4, -0.4)$ , and QUAD (blue) can generate higher-reward actions that remain within the  
 238 behavior support (black circle). Uncertainty tends to be larger when there is a significant discrep-  
 239 ency between the predicted Q-gradient (red or white arrow) and the ground-truth Q-gradient (black  
 240 arrow).  
 241

### 242 3.1.2 UNCERTAINTY-AWARE WEIGHTING IN PRACTICE

243 Although  $\lambda^*$  provides the **optimal weighting** for the abstract **Q-gradient uncertainty** model above,  
 244 it depends on the unknown quantities  $g^*$  and  $b$ , which are not identifiable from data. In practice, we  
 245 rely on a Q-ensemble to obtain multiple Q-gradient estimates and use their variance to approximate  
 246 the Q-gradient uncertainty.

247 Concretely, the variance of the projected gradients along  $\epsilon_\theta$  can be estimated from the ensemble as

$$248 \quad v^2(\mathbf{s}, \mathbf{a}^t, t) = \text{Var}(\epsilon_\theta(\mathbf{s}, \mathbf{a}^t, t) \cdot \mathbf{g}_{\phi_k}(\mathbf{s}, \mathbf{a}^t)), \quad (16)$$

249 where the variance is taken over the ensemble index  $k$ , and  $v^2$  serves as a practical estimate of the  
 250 Q-gradient uncertainty at  $(\mathbf{s}, \mathbf{a}^t, t)$ . Empirically (see Figure 3),  $v^2(\mathbf{s}, \mathbf{a}^t, t)$  is small to moderate  
 251 when the learned Q-gradients are directionally aligned with the oracle gradient, and becomes large  
 252 when different critics disagree strongly or the mean direction is misaligned.

253 These observations support a *variance-only* weighting principle: we discard the unidentifiable term  
 254 and let the per-sample weight be a monotone decreasing function of  $v^2(\mathbf{s}, \mathbf{a}^t, t)$ ,

$$255 \quad \lambda(\mathbf{s}, \mathbf{a}^t, t) = f(v^2(\mathbf{s}, \mathbf{a}^t, t)), \quad (17)$$

256 where  $f : [0, \infty) \rightarrow (0, 1]$ . In QUAD we instantiate  $f$  as an exponential:  
 257

$$258 \quad \lambda(\mathbf{s}, \mathbf{a}^t, t) = \exp\left(-\frac{v^2(\mathbf{s}, \mathbf{a}^t, t)}{\tau}\right), \quad \tau > 0. \quad (18)$$

This choice has several benefits: (i) it guarantees  $\lambda \in (0, 1]$  and thus avoids negative or overly large weights in the misaligned regime; (ii) for small variance, a first-order expansion gives  $\lambda \approx 1 - v^2/\tau$ , matching the desired shrinkage behavior of the oracle solution in the aligned regime; (iii) when the ensemble variance is large, as in the wrong-direction regime, Equation (18) drives  $\lambda$  close to zero and effectively turns off misleading critic guidance; and (iv) the exponential map is smooth and numerically stable, making it easy to tune in diffusion policy training.

### 3.2 DIFFUSION POLICY WITH Q-GRADIENT UNCERTAINTY-AWARE GUIDANCE

Building on the above analysis, we implement QUAD by integrating the uncertainty-aware weighting  $\lambda(\mathbf{s}, \mathbf{a}^t, t)$  into the diffusion policy training objective Equation (8), following the DAC framework:

$$\begin{aligned} \mathcal{L}(\theta) = & \mathbb{E}_{(\mathbf{s}, \mathbf{a}^*) \sim \mathcal{D}, t \sim \mathcal{U}(1, T), \epsilon \sim \mathcal{N}(\mathbf{0}, \mathbf{I})} \left[ \eta \|\epsilon - \epsilon_\theta(\mathbf{a}^t, \mathbf{s}, t)\|^2 \right. \\ & \left. + \lambda(\mathbf{s}, \mathbf{a}^t, t) \cdot w(t) \cdot \epsilon_\theta(\mathbf{a}^t, \mathbf{s}, t) \cdot \nabla_{\mathbf{a}^t} \hat{Q}_\phi(\mathbf{s}, \mathbf{a}^t) \right], \end{aligned} \quad (19)$$

where  $w(t) = \sqrt{1 - \bar{\alpha}_t}$  modulates the strength of Q-guidance according to the noise level, ensuring that the denoised action remains close to the behavior policy in later diffusion steps.

A central component of QUAD is the Q-ensemble, which provides diverse and informative gradient estimates and enables approximation of epistemic uncertainty in the biased-noisy model. Concretely, we maintain  $K$  parameterized Q-networks  $\{Q_{\phi_k}\}_{k=1}^K$  with corresponding target networks  $\{\hat{Q}_{\phi_k}\}_{k=1}^K$ . To reduce overestimation and better capture epistemic uncertainty, we train this ensemble using a pessimistic Q-learning scheme (Ghasemipour et al., 2022). We adopt a lower confidence bound (LCB) as the target value and optimize each critic with the loss

$$\begin{aligned} \mathcal{L}(\phi_i) = & \mathbb{E}_{(\mathbf{s}, \mathbf{a}, \mathbf{r}, \mathbf{s}') \sim \mathcal{D}, \mathbf{a}' \sim \pi_\theta} [r + \gamma Q_{\text{LCB}}(\mathbf{s}', \mathbf{a}') - Q_{\phi_i}(\mathbf{s}, \mathbf{a})]^2, \\ Q_{\text{LCB}}(\mathbf{s}', \mathbf{a}') = & \mathbb{E}[\hat{Q}(\mathbf{s}', \mathbf{a}')] - \rho \sqrt{\text{Var}[\hat{Q}(\mathbf{s}', \mathbf{a}')]}, \end{aligned} \quad (20)$$

where  $\rho \geq 0$  controls the degree of pessimism, and  $\mathbb{E}[\hat{Q}]$  and  $\text{Var}[\hat{Q}]$  denote the empirical mean and variance across the target critics.

Subsequently, given a pair  $(\mathbf{s}, \mathbf{a})$  sampled from  $\mathcal{D}$ , we add noise to the action following Equation (5) to obtain  $(\mathbf{s}, \mathbf{a}^t)$ . We then compute the ensemble alignment loss  $\{g_{\phi_k} = \epsilon_\theta \cdot \nabla_{\mathbf{a}^t} Q_{\phi_k}\}_{k=1}^K$ . Next, we estimate the heteroscedastic Q-gradient uncertainty at  $(\mathbf{s}, \mathbf{a}^t)$  via the empirical variance of this ensemble alignment loss:

$$v_\phi^2 = \frac{1}{K} \sum_{k=1}^K (g_{\phi_k} - \bar{g}_\phi)^2, \quad \bar{g}_\phi = \frac{1}{K} \sum_{k=1}^K g_{\phi_k}. \quad (21)$$

This variance  $v_\phi^2$  approximates the theoretical quantity  $v^2$  in Equation (16) under the biased-noisy model and serves as a data-driven estimate of the critic's epistemic uncertainty along the policy update direction. Finally, we plug  $v_\phi^2$  into the exponential variance-only rule Equation (18) to obtain the per-sample weight  $\lambda(\mathbf{s}, \mathbf{a}^t, t)$ , which scales the Q-gradient guidance term in Equation (19). The complete QUAD training procedure is summarized in Algorithm 1.

### 3.3 POLICY EXTRACTION

We denote  $\pi_\theta(\mathbf{a}|\mathbf{s})$  as the diffusion policy trained via the denoising process with noise predictor  $\epsilon_\theta(\mathbf{a}^t, \mathbf{s}, t)$ . While  $\pi_\theta$  can directly generate actions, we further aim to reduce uncertainty during evaluation. To this end, we draw a small batch of  $N_a$  candidate actions from  $\pi_\theta(\cdot|\mathbf{s})$  and select the one with the highest ensemble-mean Q-value:

$$\pi^*(\mathbf{s}) = \arg \max_{\mathbf{a}_1, \dots, \mathbf{a}_{N_a} \sim \pi_\theta(\cdot|\mathbf{s})} \mathbb{E}[\hat{Q}(\mathbf{s}, \mathbf{a})]. \quad (22)$$

This extraction strategy is commonly employed in settings where a stochastic actor is used for critic learning, but a deterministic policy is deployed at evaluation. Because  $\pi_\theta$  is already trained to approximate the target policy, only a small number of samples  $N_a$  is needed. In our experiments, QUAD achieves strong performance with  $N_a = 10$  following DAC, whereas SfBC and Diffusion Q-learning typically require  $N_a = 32$  and  $N_a = 50$ , respectively.

324 

## 4 RELATED WORK

325 

### 4.1 OFFLINE RL

328 Offline RL aims to learn policies from fixed datasets, but suffers from distribution shift that leads to  
 329 value overestimation in the bootstrapping process (Levine et al., 2020). To address this issue, prior  
 330 works have developed strategies such as behavior regularization, conservative value estimation, and  
 331 explicit Bellman error modeling. Behavior-regularized methods constrain policies to stay close to  
 332 the behavior distribution via candidate-action generators or divergence penalties (Fujimoto et al.,  
 333 2019; Kumar et al., 2019; Wu et al., 2019). Conservative methods alleviate OOD effects by either  
 334 adding regularizers to the Q-learning objective (Kumar et al., 2020) or by learning in-sample con-  
 335 servative value functions (Kostrikov et al., 2021; Xu et al., 2023). Alternative approaches explicitly  
 336 model Bellman errors with a Gumbel distribution and directly learn soft value functions without  
 337 requiring action sampling (Garg et al., 2023). Our work is related to both behavior-regularized and  
 338 conservative approaches, as we model the behavior distribution with a diffusion policy and mitigate  
 339 overestimation bias via a pessimistic Q-ensemble.

340 

### 4.2 DIFFUSION MODELS

342 Diffusion models are a class of generative models that consist of a forward diffusion process and a  
 343 reverse denoising process (Ho et al., 2020), which can also be interpreted as stochastic differential  
 344 equations (Song et al., 2020b). In the forward process, Gaussian noise is gradually added to the  
 345 data according to a variance schedule. In the reverse process, a neural network is trained to predict  
 346 the noise and iteratively recover the clean data. Several works improve efficiency by reducing the  
 347 number of denoising steps (Song et al., 2020a; Nichol & Dhariwal, 2021; Song et al., 2023). Others  
 348 explore alternative guidance strategies, such as classifier guidance (Dhariwal & Nichol, 2021) and  
 349 classifier-free guidance (Ho & Salimans, 2022). More recently, diffusion models have been extended  
 350 to sequential decision-making, where they are used to represent policies or trajectories (Janner et al.,  
 351 2022; Chi et al., 2023; Black et al., 2023). Our work builds on diffusion policies and introduces a  
 352 novel uncertainty-aware Q-gradient mechanism to enhance policy learning in offline RL.

353 

### 4.3 DIFFUSION-BASED OFFLINE RL

354 Diffusion-based offline RL combines diffusion models with offline RL techniques. A straightfor-  
 355 ward approach performs behavior cloning with diffusion models and then applies value-based se-  
 356 lection to choose high-value actions from the diffusion prior (Chen et al., 2022; Hansen-Estruch  
 357 et al., 2023). To reduce multi-step sampling cost, an efficient variant distills the diffusion prior into  
 358 a one-step Gaussian policy (Chen et al., 2024). Another line of work integrates Q-value infor-  
 359 mation directly into diffusion policy training (Wang et al., 2022). However, this approach requires  
 360 backpropagating Q-gradients through the entire denoising chain, which often causes vanishing or  
 361 exploding gradients. A more refined strategy applies Q-gradient guidance at each intermediate de-  
 362 noising step, rather than through all steps, as in DAC (Fang et al., 2024). Subsequent extensions  
 363 incorporate advantage modules or pathwise regularization to further stabilize training (Chen et al.,  
 364 2025; Gao et al., 2025). Despite their improved stability, these methods still suffer from unreli-  
 365 able Q-gradients when noisy actions deviate from the dataset distribution. Our method addresses  
 366 this limitation by employing a Q-ensemble to estimate gradient uncertainty and suppress unreliable  
 367 guidance, thereby improving the robustness of diffusion-based offline RL.

368 

## 5 EXPERIMENTS

369 In our experiments, we aim to address the following questions:

- 370 • Does QUAD outperform state-of-the-art offline RL methods across diverse tasks?
- 371 • What is the effect of uncertainty-aware weighting on policy learning and performance?
- 372 • How sensitive is QUAD to the choice of uncertainty temperature  $\tau$ ?

378  
379

## 5.1 SETUP

380  
381  
382  
383  
384  
385  
386

**Offline Datasets.** We evaluate QUAD on the widely used D4RL benchmark (Fu et al., 2020), which covers a variety of continuous control tasks with different dataset compositions. Specifically, we consider standard locomotion tasks (HalfCheetah, Hopper, Walker2d) and the more challenging AntMaze tasks. For locomotion, we use version “v0” datasets of three quality levels: medium (m), medium-replay (m-r), and medium-expert (m-e). For AntMaze, we use version “v2” datasets: umaze (u), umaze-diverse (u-div), medium-play (m-play), medium-diverse (m-div), large-play (l-play), and large-diverse (l-div).

387  
388  
389  
390  
391  
392

**Baselines.** We compare QUAD against a range of offline RL methods, including both non-diffusion and diffusion-based approaches. Non-diffusion baselines include One-step RL (Brandfonbrener et al., 2021), CQL (Kumar et al., 2020), IQL (Kostrikov et al., 2021), IVR (Xu et al., 2023) and EQL (Garg et al., 2023). Diffusion-based baselines include, Diffuser (Janner et al., 2022), SfBC (Chen et al., 2022), Diffusion Q-learning (DQL) (Wang et al., 2022), DTQL (Chen et al., 2024), AlignIQL (He et al., 2024a), and DAC (Fang et al., 2024).

393  
394  
395  
396  
397  
398  
399  
400  
401  
402

**Implementation Details.** We implement QUAD on top of the publicly available DAC codebase (Fang et al., 2024). For fair comparison, we adopt the same network architectures and hyperparameters as DAC for both the diffusion policy and the Q-ensemble, unless otherwise specified. We set the ensemble size to  $K = 10$  and the temperature to  $\tau = 1.0$  for uncertainty weighting, based on preliminary tuning. All models are trained for 2 million gradient steps and evaluated every 20,000 steps using 10 episodes per evaluation. We report the average normalized scores over 4 random seeds for each task, and the final results are averaged over the last 5 evaluations, which typically exhibit stable performance, following the DAC protocol. For baselines, we use the results reported in their respective papers. A complete summary of experimental configurations is provided in Appendix B.

403  
404

## 5.2 MAIN RESULTS

405  
406  
407  
408  
409  
410  
411

As shown in Table 1, QUAD outperforms most baselines across a variety of tasks, demonstrating the effectiveness of uncertainty-aware weighting and Q-ensemble learning. We also observe that QUAD does not achieve the best performance on AntMaze “large” tasks, where the challenges of sparse rewards and limited optimal trajectories persist. We hypothesize that in these datasets, learning a reliable critic is particularly difficult, making uncertainty-aware weighting unstable and revealing an important limitation of QUAD.

412  
413

Table 1: **Average normalized scores of QUAD vs. baselines.** Abbreviations: “m” = medium, “r” = replay, “e” = expert, “u” = umaze, “div” = diverse, “l” = large. Bold numbers denote the best scores, or the second-best if achieved by our method.

Dataset	Onestep-RL	CQL	IQL	IVR	EQL	Diffuser	DTQL	AlignIQL	SfBC	DQL	DAC	QUAD (ours)
halfcheetah-m	48.4	44.0	47.4	48.3	48.3	44.2	57.9	46.0	45.9	51.1	59.1	<b>59.2</b> $\pm$ 0.2
hopper-m	59.6	58.5	66.3	75.5	74.2	58.5	99.6	56.1	57.1	90.5	<b>101.2</b>	<b>100.2</b> $\pm$ 3.5
walker2d-m	81.8	72.5	78.3	84.2	84.2	79.7	89.4	78.5	77.9	87.0	96.8	<b>100.7</b> $\pm$ 2.4
halfcheetah-m-r	38.1	45.5	44.2	44.8	45.2	42.2	50.9	41.1	37.1	47.8	55.0	<b>55.5</b> $\pm$ 0.3
hopper-m-r	97.5	95.0	94.7	99.7	100.7	96.8	100.0	74.8	86.2	101.3	103.1	<b>103.6</b> $\pm$ 0.2
walker2d-m-r	49.5	77.2	73.9	81.2	82.2	61.2	88.5	76.5	65.1	95.5	96.8	<b>98.9</b> $\pm$ 1.0
halfcheetah-m-e	93.4	91.6	86.7	94.0	94.2	79.8	92.7	89.1	92.6	96.8	99.1	<b>100.1</b> $\pm$ 0.4
hopper-m-e	103.3	105.4	91.5	111.8	111.2	107.2	109.3	107.1	108.6	111.1	111.7	<b>111.9</b> $\pm$ 0.4
walker2d-m-e	113.0	108.8	109.6	110.2	112.7	108.4	110.0	111.9	109.8	110.1	113.6	<b>115.5</b> $\pm$ 1.0
<b>locomotion total</b>	684.6	698.5	749.7	749.7	752.9	678.0	798.3	681.1	680.3	791.2	836.4	<b>845.6</b>
antmaze-u	64.3	74.0	87.5	93.2	93.8	-	94.8	94.8	92.0	93.4	99.5	<b>100.0</b> $\pm$ 0.0
antmaze-u-div	60.7	84.0	62.2	74.0	82.0	-	78.8	82.4	85.3	66.2	85.0	<b>85.5</b> $\pm$ 16.5
antmaze-m-play	0.3	61.2	71.2	80.2	76.0	-	79.6	80.5	81.3	76.6	85.8	<b>93.0</b> $\pm$ 3.3
antmaze-m-div	0.0	53.7	70.0	79.1	73.6	-	82.2	85.5	82.0	78.6	84.0	<b>89.5</b> $\pm$ 2.6
antmaze-l-play	0.0	15.8	39.6	53.2	46.5	-	52.0	<b>65.2</b>	59.3	46.4	50.3	<b>60.0</b> $\pm$ 4.2
antmaze-l-div	0.0	14.9	47.5	52.3	49.0	-	<b>66.4</b>	54.0	45.5	56.6	55.3	50.5 $\pm$ 19.5
<b>antmaze total</b>	125.3	303.6	378.0	432.0	420.9	-	441.4	474.8	445.4	417.8	459.9	<b>479.0</b>

431

432 5.3 ABLATION STUDIES  
433

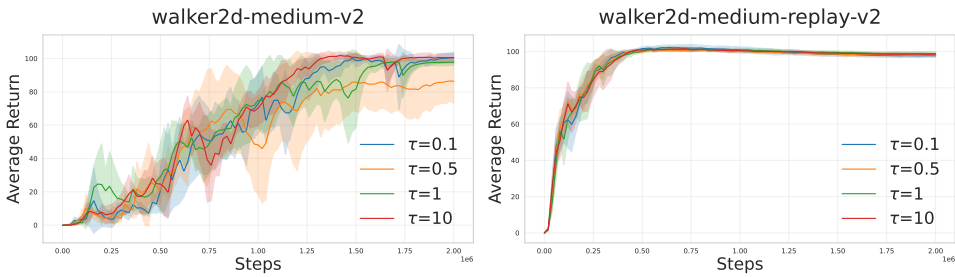
434 Since our method builds on DAC, which can be viewed as an unweighted variant of QUAD, we  
435 reproduce DAC using the same codebase and training protocol as QUAD, denoted as DAC-Rep. We  
436 evaluate both methods on locomotion tasks with “medium-replay” datasets and AntMaze “medium”  
437 and “large” tasks, as these settings are highly representative of dense- and sparse-reward regimes, re-  
438 spectively. All hyperparameters are kept identical except for those related to uncertainty modeling.  
439 As shown in Table 2, QUAD consistently outperforms DAC-Rep across these tasks, highlighting  
440 the effectiveness of uncertainty weighting. These improvements stem from QUAD’s ability to mit-  
441 iate the adverse effects of unreliable Q-gradients. The gains are particularly pronounced in the  
442 challenging AntMaze tasks, where Q-gradients are especially uncertain during denoising.  
443

444 Table 2: Uncertainty weight ablation on locomotion “medium-replay” datasets and AntMaze  
445 “medium”/“large” tasks, comparing QUAD with its unweighted variant DAC-Rep. QUAD achieves  
446 higher returns, especially on AntMaze where Q-gradients are highly uncertain.

447 uncertainty weight	walker2d	hopper	halfcheetah	antmaze			
	m-r	m-r	m-r	m-p	m-d	l-p	l-d
449 w/o. (DAC-Rep)	98.1 $\pm$ 1.5	103.4 $\pm$ 0.2	55.3 $\pm$ 0.2	88.5 $\pm$ 3.0	82.5 $\pm$ 17.7	41.5 $\pm$ 24.4	42.5 $\pm$ 11.1
450 w. (QUAD)	<b>98.9 <math>\pm</math> 1.0</b>	<b>103.6 <math>\pm</math> 0.2</b>	<b>55.5 <math>\pm</math> 0.3</b>	<b>93.0 <math>\pm</math> 3.3</b>	<b>89.5 <math>\pm</math> 2.6</b>	<b>60.0 <math>\pm</math> 4.2</b>	<b>50.5 <math>\pm</math> 19.5</b>

## 451 452 453 454 5.4 SENSITIVITY ANALYSIS

455 To examine the sensitivity of QUAD to key hyperparameters, we vary the uncertainty tempera-  
456 ture  $\tau \in \{0.1, 0.5, 1.0, 10.0\}$ . We present results on “walker2d-medium” and “walker2d-medium-  
457 replay” in Figure 4, while full tasks are reported in Appendix B.4. Our findings indicate that QUAD  
458 is more sensitive to  $\tau$  in “medium” than in “medium-replay”, likely because the former exhibits a  
459 narrower data distribution, making uncertainty estimates less reliable than in “medium-replay”.



470 Figure 4: Sensitivity of QUAD to uncertainty temperature  $\tau$ , with stronger effects in “medium” due  
471 to its narrower data distribution.

472 473 474 6 CONCLUSION  
475

476 We introduced QUAD, a diffusion-based offline RL method that incorporates uncertainty-aware Q-  
477 gradient weighting to improve policy learning. By leveraging a Q-ensemble to estimate uncertainty,  
478 QUAD mitigates the adverse effects of unreliable Q-gradients during denoising. Our theoretical  
479 analysis shows that this weighting scheme stabilizes optimization and enhances policy performance.  
480 Extensive experiments on the D4RL benchmark demonstrate that QUAD outperforms state-of-the-  
481 art diffusion-based methods across diverse tasks, particularly in challenging high-uncertainty set-  
482 tings. A limitation of QUAD lies in its reliance on the variance of Q-ensemble gradients for uncer-  
483 tainty estimation. The diversity of the Q-ensemble is also crucial for reliable uncertainty estimates,  
484 which may benefit from techniques such as data augmentation or ensemble diversity promotion. Fu-  
485 ture work includes exploring more advanced uncertainty estimation methods and extending QUAD  
486 to broader RL scenarios, such as offline meta-RL.

486 REFERENCES  
487

488 Kevin Black, Michael Janner, Yilun Du, Ilya Kostrikov, and Sergey Levine. Training diffusion  
489 models with reinforcement learning. *arXiv preprint arXiv:2305.13301*, 2023.

490 David Brandfonbrener, Will Whitney, Rajesh Ranganath, and Joan Bruna. Offline rl without off-  
491 policy evaluation. *Advances in neural information processing systems*, 34:4933–4946, 2021.

492

493 Huayu Chen, Cheng Lu, Chengyang Ying, Hang Su, and Jun Zhu. Offline reinforcement learning  
494 via high-fidelity generative behavior modeling. *arXiv preprint arXiv:2209.14548*, 2022.

495 Tianyu Chen, Zhendong Wang, and Mingyuan Zhou. Diffusion policies creating a trust region for  
496 offline reinforcement learning. *Advances in Neural Information Processing Systems*, 37:50098–  
497 50125, 2024.

498

499 Xuyang Chen, Keyu Yan, and Lin Zhao. Taming ood actions for offline reinforcement learning: An  
500 advantage-based approach. *arXiv preprint arXiv:2505.05126*, 2025.

501

502 Cheng Chi, Zhenjia Xu, Siyuan Feng, Eric Cousineau, Yilun Du, Benjamin Burchfiel, Russ Tedrake,  
503 and Shuran Song. Diffusion policy: Visuomotor policy learning via action diffusion. *The Inter-  
504 national Journal of Robotics Research*, pp. 02783649241273668, 2023.

505

506 Prafulla Dhariwal and Alexander Nichol. Diffusion models beat gans on image synthesis. *Advances  
507 in neural information processing systems*, 34:8780–8794, 2021.

508

509 Linjiajie Fang, Ruoxue Liu, Jing Zhang, Wenjia Wang, and Bing-Yi Jing. Diffusion actor-critic:  
510 Formulating constrained policy iteration as diffusion noise regression for offline reinforcement  
511 learning. *arXiv preprint arXiv:2405.20555*, 2024.

512

513 Justin Fu, Aviral Kumar, Ofir Nachum, George Tucker, and Sergey Levine. D4rl: Datasets for deep  
514 data-driven reinforcement learning. *arXiv preprint arXiv:2004.07219*, 2020.

515

516 Scott Fujimoto and Shixiang Shane Gu. A minimalist approach to offline reinforcement learning.  
517 *Advances in neural information processing systems*, 34:20132–20145, 2021.

518

519 Scott Fujimoto, Edoardo Conti, Mohammad Ghavamzadeh, and Joelle Pineau. Benchmarking batch  
520 deep reinforcement learning algorithms. *arXiv preprint arXiv:1910.01708*, 2019.

521

522 Chen-Xiao Gao, Chenyang Wu, Mingjun Cao, Chenjun Xiao, Yang Yu, and Zongzhang Zhang.  
523 Behavior-regularized diffusion policy optimization for offline reinforcement learning. *arXiv  
524 preprint arXiv:2502.04778*, 2025.

525

526 Divyansh Garg, Joey Hejna, Matthieu Geist, and Stefano Ermon. Extreme q-learning: Maxent rl  
527 without entropy. *arXiv preprint arXiv:2301.02328*, 2023.

528

529 Kamyar Ghasemipour, Shixiang Shane Gu, and Ofir Nachum. Why so pessimistic? estimating  
530 uncertainties for offline rl through ensembles, and why their independence matters. *Advances in  
531 Neural Information Processing Systems*, 35:18267–18281, 2022.

532

533 Philippe Hansen-Estruch, Ilya Kostrikov, Michael Janner, Jakub Grudzien Kuba, and Sergey Levine.  
534 Idql: Implicit q-learning as an actor-critic method with diffusion policies. *arXiv preprint  
535 arXiv:2304.10573*, 2023.

536

537 Longxiang He, Li Shen, Junbo Tan, and Xueqian Wang. Aligniql: Policy alignment in implicit  
538 q-learning through constrained optimization. *arXiv preprint arXiv:2405.18187*, 2024a.

539

540 Tairan He, Zhengyi Luo, Xialin He, Wenli Xiao, Chong Zhang, Weinan Zhang, Kris Kitani,  
541 Changliu Liu, and Guanya Shi. Omnih2o: Universal and dexterous human-to-humanoid whole-  
542 body teleoperation and learning. *arXiv preprint arXiv:2406.08858*, 2024b.

543

544 Jonathan Ho and Tim Salimans. Classifier-free diffusion guidance. *arXiv preprint  
545 arXiv:2207.12598*, 2022.

546

547 Jonathan Ho, Ajay Jain, and Pieter Abbeel. Denoising diffusion probabilistic models. *Advances in  
548 neural information processing systems*, 33:6840–6851, 2020.

540 Michael Janner, Yilun Du, Joshua B Tenenbaum, and Sergey Levine. Planning with diffusion for  
 541 flexible behavior synthesis. *arXiv preprint arXiv:2205.09991*, 2022.

542

543 Ilya Kostrikov. JAXRL: Implementations of Reinforcement Learning algorithms in JAX, 10 2021.  
 544 URL <https://github.com/ikostrikov/jaxrl>.

545

546 Ilya Kostrikov, Ashvin Nair, and Sergey Levine. Offline reinforcement learning with implicit q-  
 547 learning. *arXiv preprint arXiv:2110.06169*, 2021.

548

549 Aviral Kumar, Justin Fu, Matthew Soh, George Tucker, and Sergey Levine. Stabilizing off-policy  
 550 q-learning via bootstrapping error reduction. *Advances in neural information processing systems*,  
 551 32, 2019.

552

553 Aviral Kumar, Aurick Zhou, George Tucker, and Sergey Levine. Conservative q-learning for offline  
 554 reinforcement learning. *Advances in neural information processing systems*, 33:1179–1191, 2020.

555

556 Guillaume Lample and Devendra Singh Chaplot. Playing fps games with deep reinforcement learn-  
 557 ing. In *Proceedings of the AAAI conference on artificial intelligence*, volume 31, 2017.

558

559 Sergey Levine, Aviral Kumar, George Tucker, and Justin Fu. Offline reinforcement learning: Tuto-  
 560 rial, review, and perspectives on open problems. *arXiv preprint arXiv:2005.01643*, 2020.

561

562 Misra D Mish. A self regularized non-monotonic activation function. 2019. *arXiv preprint*  
 563 *arXiv:1908.08681*, 1908.

564

565 Volodymyr Mnih, Koray Kavukcuoglu, David Silver, Alex Graves, Ioannis Antonoglou, Daan Wier-  
 566 stra, and Martin Riedmiller. Playing atari with deep reinforcement learning. *arXiv preprint*  
 567 *arXiv:1312.5602*, 2013.

568

569 Alexander Quinn Nichol and Prafulla Dhariwal. Improved denoising diffusion probabilistic models.  
 570 In *International conference on machine learning*, pp. 8162–8171. PMLR, 2021.

571

572 Jiaming Song, Chenlin Meng, and Stefano Ermon. Denoising diffusion implicit models. *arXiv*  
 573 *preprint arXiv:2010.02502*, 2020a.

574

575 Yang Song, Jascha Sohl-Dickstein, Diederik P Kingma, Abhishek Kumar, Stefano Ermon, and Ben  
 576 Poole. Score-based generative modeling through stochastic differential equations. *arXiv preprint*  
 577 *arXiv:2011.13456*, 2020b.

578

579 Yang Song, Prafulla Dhariwal, Mark Chen, and Ilya Sutskever. Consistency models. 2023.

580

581 Richard S Sutton, Andrew G Barto, et al. *Reinforcement learning: An introduction*, volume 1. MIT  
 582 press Cambridge, 1998.

583

584 Zhendong Wang, Jonathan J Hunt, and Mingyuan Zhou. Diffusion policies as an expressive policy  
 585 class for offline reinforcement learning. *arXiv preprint arXiv:2208.06193*, 2022.

586

587 Yifan Wu, George Tucker, and Ofir Nachum. Behavior regularized offline reinforcement learning.  
 588 *arXiv preprint arXiv:1911.11361*, 2019.

589

590 Haoran Xu, Li Jiang, Jianxiong Li, Zhuoran Yang, Zhaoran Wang, Victor Wai Kin Chan, and Xi-  
 591 anyuan Zhan. Offline rl with no ood actions: In-sample learning via implicit value regularization.  
 592 *arXiv preprint arXiv:2303.15810*, 2023.

593

594 Yanjie Ze, Zixuan Chen, JoĂš Go Pedro AraĂšjo, Zi-ang Cao, Xue Bin Peng, Jiajun Wu, and C Karen  
 595 Liu. Twist: Teleoperated whole-body imitation system. *arXiv preprint arXiv:2505.02833*, 2025.

596

597 Hongtu Zhou, Ruiling Yang, Yakun Zhu, Haoqi Zhao, Hai Zhang, Di Zhang, Junqiao Zhao, Chen Ye,  
 598 and Changjun Jiang. Certain: Context uncertainty-aware one-shot adaptation for context-based  
 599 offline meta reinforcement learning. In *International conference on machine learning*, 2025.

600

594 THE USE OF LLMs  
595596 We thank ChatGPT-5 for its assistance in polishing the writing and proofreading of this paper. The  
597 authors are responsible for the content and presentation.  
598599 A DETAILED PROOFS AND EXTENSIONS OF QUAD THEORY  
600601 In this appendix we complement Section 3.1 by (i) deriving the closed-form **optimal weighting**  $\lambda^*$   
602 for the biased–noisy scalar model, and (ii) explaining how the ensemble variance  $v^2(s, a^t, t)$  used  
603 in practice approximates the theoretical **Q-gradient uncertainty** modeled in the main text.  
604605 A.1 DERIVATION OF THE OPTIMAL WEIGHTING  
606607 In the main text we work with scalar alignment losses  
608

609 
$$g^* \triangleq \epsilon_\theta \cdot \mathbf{g}^*, \quad g_\phi \triangleq \epsilon_\theta \cdot \mathbf{g}_\phi,$$

610 and assume the biased–noisy decomposition  
611

612 
$$g_\phi = g^* + b + \xi_\phi,$$

613 where  $b$  is a deterministic bias determined only by the offline dataset and the learning algorithm, and  
614  $\xi_\phi$  is a zero-mean random noise with finite variance  $\sigma^2(s, a^t, t)$ , arising from stochastic function  
615 approximation and training randomness. For a fixed  $(s, a^t, t)$  we drop the arguments and simply  
616 write  $g^*, b, \xi, \sigma^2$ .617 The main text defines the alignment risk  
618

619 
$$\mathcal{R} \triangleq \mathbb{E}[(g_\phi - g^*)^2],$$

620 and, for a per-sample weight  $\lambda$ , the weighted risk  
621

622 
$$\mathcal{R}(\lambda) \triangleq \mathbb{E}[(\lambda g_\phi - g^*)^2].$$

623 Substituting  $g_\phi = g^* + b + \xi$  gives  
624

625 
$$\mathcal{R}(\lambda) = \mathbb{E}[(\lambda(g^* + b + \xi) - g^*)^2]. \quad (23)$$

626 We now expand Equation (23) step by step. Write  
627

628 
$$\lambda(g^* + b + \xi) - g^* = (\lambda(g^* + b) - g^*) + \lambda\xi,$$

629 so that  
630

631 
$$\mathcal{R}(\lambda) = \mathbb{E}[(\lambda(g^* + b) - g^* + \lambda\xi)^2].$$

632 Using  $(x + y)^2 = x^2 + 2xy + y^2$  with  
633

634 
$$x = \lambda(g^* + b) - g^*, \quad y = \lambda\xi,$$

635 we obtain  
636

637 
$$\mathcal{R}(\lambda) = x^2 + 2x\mathbb{E}[y] + \mathbb{E}[y^2].$$

638 Since  $\mathbb{E}[\xi] = 0$  and  $\mathbb{E}[\xi^2] = \sigma^2$ , we have  $\mathbb{E}[y] = \lambda\mathbb{E}[\xi] = 0$  and  $\mathbb{E}[y^2] = \lambda^2\sigma^2$ , hence  
639

640 
$$\mathcal{R}(\lambda) = (\lambda(g^* + b) - g^*)^2 + \lambda^2\sigma^2. \quad (24)$$

641 Expanding the first term in Equation (24) yields  
642

643 
$$(\lambda(g^* + b) - g^*)^2 = \lambda^2(g^* + b)^2 - 2\lambda g^*(g^* + b) + (g^*)^2,$$

644 so  
645

646 
$$\begin{aligned} \mathcal{R}(\lambda) &= \lambda^2(g^* + b)^2 - 2\lambda g^*(g^* + b) + (g^*)^2 + \lambda^2\sigma^2 \\ &= ((g^* + b)^2 + \sigma^2)\lambda^2 - 2g^*(g^* + b)\lambda + (g^*)^2. \end{aligned} \quad (25)$$

647 This is a quadratic function of  $\lambda$  with positive leading coefficient  $(g^* + b)^2 + \sigma^2 > 0$ , so it is strictly  
648 convex.

648 Taking the derivative of Equation (25) with respect to  $\lambda$  and setting it to zero:  
 649  
 650

$$\frac{\partial \mathcal{R}(\lambda)}{\partial \lambda} = 2((g^* + b)^2 + \sigma^2)\lambda - 2g^*(g^* + b) = 0,$$

651 we obtain the **optimal weighting**

$$\lambda^* = \frac{g^*(g^* + b)}{(g^* + b)^2 + \sigma^2}, \quad (26)$$

652 which is exactly the form used in the main text (with the dependence on  $(s, a^t, t)$  made explicit  
 653 there).  
 654

655 For completeness, evaluating Equation (25) at  $\lambda = 1$  gives  
 656

$$\mathcal{R}(1) = (g^* + b)^2 + \sigma^2 - 2g^*(g^* + b) + (g^*)^2 = b^2 + \sigma^2.$$

657 Since Equation (25) is strictly convex and minimized at  $\lambda^*$ , we have  $\mathcal{R}(\lambda^*) \leq \mathcal{R}(1) = b^2 + \sigma^2$ ,  
 658 showing that there always exists a scalar weight that performs no worse (in alignment risk) than  
 659 using the unweighted critic.  
 660

## 661 A.2 WHAT DOES THE ENSEMBLE CAPTURE, AND HOW TO USE IT IN PRACTICE?

662 The scalar model in Section 3.1 parameterizes the **Q-gradient uncertainty** at a given  $(s, a^t, t)$  by a  
 663 deterministic bias  $b$  and a noise term  $\xi$  through  
 664

$$g_\phi = g^* + b + \xi,$$

665 where  $b$  is a deterministic bias determined only by the offline dataset and the learning algorithm, and  
 666  $\xi$  is zero-mean random noise with variance  $\sigma^2(s, a^t, t) = \text{Var}(\xi)$ , arising from stochastic function  
 667 approximation and training randomness rather than from the fixed data or algorithm design. The  
 668 combined term  $b + \xi$  captures the epistemic uncertainty of the Q-gradient, which we refer to as the  
 669 **Q-gradient uncertainty**. In this model, the **optimal weighting** in Equation (26) depends on both  $b$   
 670 and  $\sigma^2(s, a^t, t)$ .  
 671

672 In practice, QUAD cannot observe  $b$  or  $\sigma^2(s, a^t, t)$  directly, and instead uses a Q-ensemble to ap-  
 673 proximate the **Q-gradient uncertainty**. We maintain  $K$  critics  $\{Q_{\phi_k}\}_{k=1}^K$  and define their gradient-  
 674 based alignment losses along  $\epsilon_\theta$  as  
 675

$$g_k(s, a^t, t) \triangleq \epsilon_\theta(a^t, s, t) \cdot \nabla_{a^t} Q_{\phi_k}(s, a^t), \quad k = 1, \dots, K.$$

676 Under the same biased-noisy picture, each  $g_k$  can be written as  
 677

$$g_k = g^* + b + \xi_k,$$

678 where the oracle alignment  $g^*$  and the deterministic bias  $b$  are shared across critics at  $(s, a^t, t)$ ,  
 679 while the zero-mean noises  $\xi_k$  come from the randomness of individual function approximators and  
 680 training.  
 681

682 To obtain a data-driven estimate of this noise level, we use the empirical variance of the alignment  
 683 losses across the ensemble:  
 684

$$v^2(s, a^t, t) = \frac{1}{K} \sum_{k=1}^K (g_k(s, a^t, t) - \bar{g}(s, a^t, t))^2, \quad \bar{g}(s, a^t, t) = \frac{1}{K} \sum_{k=1}^K g_k(s, a^t, t).$$

685 Under the usual assumption that the noises  $\{\xi_k\}$  are independent across  $k$ ,  $v^2(s, a^t, t)$  is a standard  
 686 sample-variance estimator of  $\text{Var}(g_k)$  and provides a practical approximation of the Q-gradient  
 687 uncertainty that appears in the **optimal weighting**  $\lambda^*$ .  
 688

689 However, the exact form of  $\lambda^*$  in Equation (26) depends on terms which are not identifiable from  
 690 data. Motivated by this, QUAD adopts a variance-only weighting rule that uses  $v^2(s, a^t, t)$  as a  
 691 surrogate for the **Q-gradient uncertainty** and defines  
 692

$$\lambda(s, a^t, t) = f(v^2(s, a^t, t)),$$

693 where  $f : [0, \infty) \rightarrow (0, 1]$  is a decreasing function. In the main text we instantiate  $f$  as the expo-  
 694 nential  
 695

$$\lambda(s, a^t, t) = \exp\left(-\frac{v^2(s, a^t, t)}{\tau}\right),$$

696 as in Equation (18). This choice preserves the qualitative behavior of the theoretical **optimal weight-  
 697 ing**: when the ensemble variance (and thus the estimated **Q-gradient uncertainty**) is small,  $\lambda$  stays  
 698 close to 1 and preserves strong Q-gradient guidance; when the ensemble variance is large,  $\lambda$  decays  
 699 towards 0 and automatically down-weights unreliable critic signals.  
 700

702 **B DETAILS OF EXPERIMENTAL SETUP**  
 703

704 We train all models for 2M gradient steps. Each environment is run with 4 independent seeds,  
 705 and performance is evaluated every 20k steps using 10 additional seeds, yielding 40 rollouts per  
 706 evaluation. We report the mean score over the final 50k steps without early stopping. Experiments  
 707 are conducted on 4 RTX 4090 GPUs, with each run taking about 2.5 hours including training and  
 708 evaluation. Our implementation builds on the jaxrl (Kostrikov, 2021) codebase.

710 **B.1 NETWORK ARCHITECTURE**  
 711

712 Both the actor and critic adopt a 3-layer MLP with hidden size 256 and Mish activation (Mish, 1908).  
 713 Target networks are used to stabilize training:  $\hat{\epsilon}_\theta$  and  $\hat{Q}_{\phi_k}$  are initialized with the same parameters  
 714 as  $\epsilon_\theta$  and  $Q_{\phi_k}$ , and track their exponential moving averages (EMA). The target actor is updated  
 715 every 5 gradient steps, while the target critics are updated after each step.

716 **B.2 HYPERPARAMETERS**  
 717

718 We use consistent hyperparameter settings for the diffusion models and networks across all tasks.  
 719 The hyperparameters are specified as follows:  
 720

721 **Table 3: Hyperparameters for all networks and tasks.**

722 <b>Hyperparameter</b>	723 <b>Value</b>
724 T (Diffusion Steps)	5
725 $\beta_t$ (Noise Schedule)	Variance Preserving ()
726 K (Ensemble Size)	10
727 B (Batch Size)	256
728 Learning Rates (for all networks)	3e-4, 1e-3 (antmaze-large)
729 Learning Rate Decay	Cosine ()
730 Optimizer	Adam ()
731 $\eta_{\text{init}}$ (Initial Behavior Cloning Strength)	[0.1, 1]
732 $\alpha_\eta$ (for Dual Gradient Ascent)	0.001
733 $\alpha_{\text{ema}}$ (EMA Learning Rate)	5e-3
734 $N_a$ (Number of sampled actions for evaluation)	10
735 $b$ (Behavior Cloning Threshold)	[0.05, 1]
736 $\rho$ (Pessimistic factor)	[0, 2]

737 QUAD adopts the same hyperparameters as DAC for the diffusion policy and Q-ensemble, except  
 738 for AntMaze “large” tasks where a smaller  $\eta$  is used. We sweep over  $\tau \in \{0.1, 0.5, 1.0, 10.0, 100\}$   
 739 and report the best value for each task in Table 4.

740 **B.3 PSEUDO CODE OF QUAD**  
 741

742 We provide the pseudo code of QUAD in Algorithm 1.

743 **B.4 SENSITIVITY ANALYSIS**  
 744

745 We present the full sensitivity analysis of QUAD to uncertainty temperature  $\tau$  on all tasks in Figure 5.  
 746

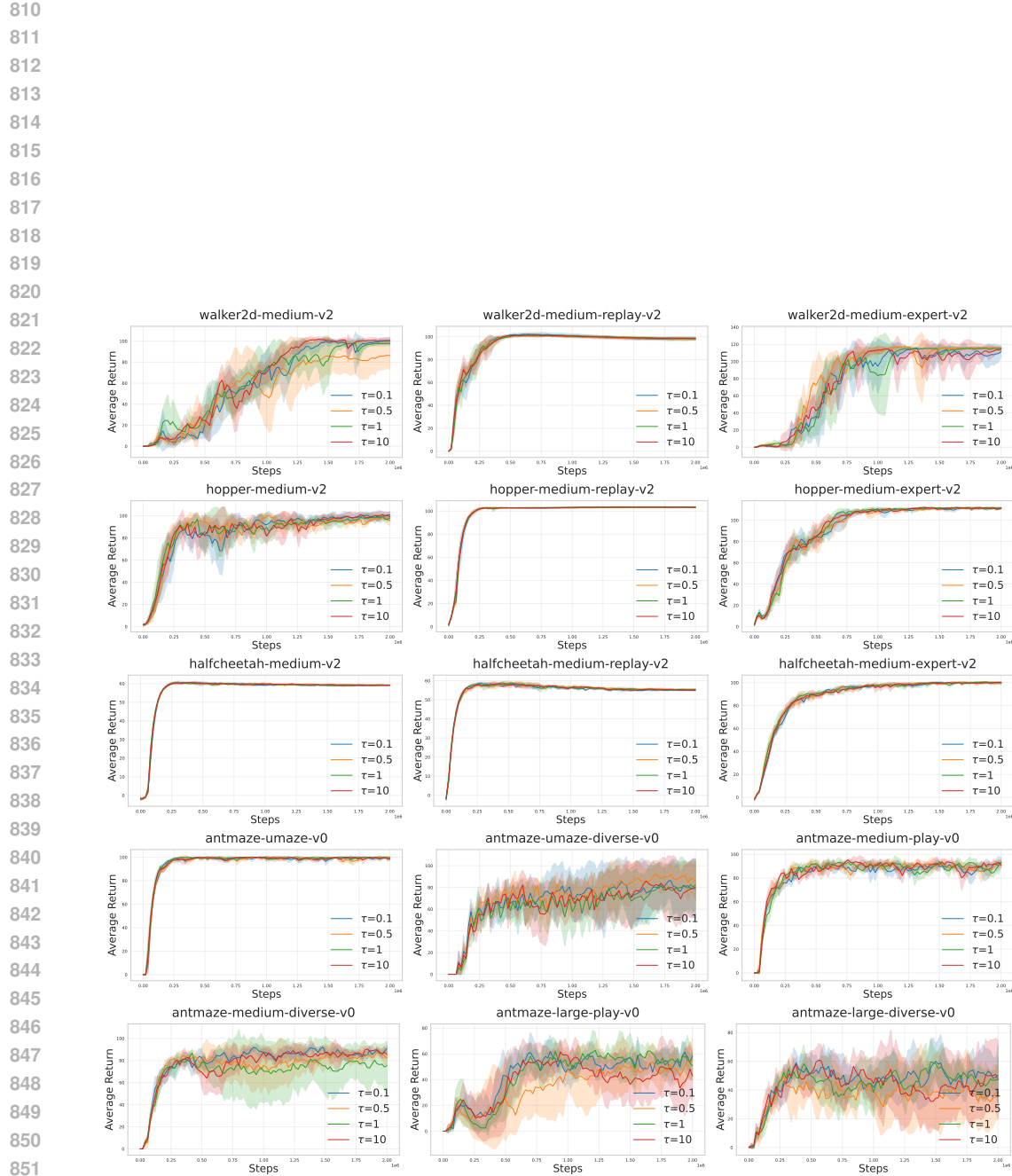
747  
 748  
 749  
 750  
 751  
 752  
 753  
 754  
 755

Table 4: Hyperparameters settings for tasks.

Tasks	$\tau$	$b$	$\eta$	$\rho$	Regularization	Type
hopper-medium-v2	0.1	1	-	1.5		Learnable
hopper-medium-replay-v2	1	1	-	1.5		Learnable
hopper-medium-expert-v2	0.5	0.05	-	1.5		Learnable
walker2d-medium-v2	10	1	-	1		Learnable
walker2d-medium-replay-v2	1	1	-	1		Learnable
walker2d-medium-expert-v2	1	1	-	1		Learnable
halfcheetah-medium-v2	10	1	-	0		Learnable
halfcheetah-medium-replay-v2	0.5	1	-	0		Learnable
halfcheetah-medium-expert-v2	10	0.1	-	0		Learnable
antmaze-umaze-v0	0.5	-	0.1	1		Constant
antmaze-umaze-diverse-v0	0.5	-	0.1	1		Constant
antmaze-medium-play-v0	0.1	-	0.1	1		Constant
antmaze-medium-diverse-v0	0.1	-	0.1	1		Constant
antmaze-large-play-v0	0.1	-	0.1	1.1		Constant
antmaze-large-diverse-v0	0.1	-	0.1	1		Constant

---

**Algorithm 1** QUAD: Q-gradient Uncertainty-aware Guidance Training

Figure 5: Sensitivity of QUAD to uncertainty temperature  $\tau$  on various tasks.